Journal of Chromatography A, 1218 (2011) 2944–2953

Contents lists available at ScienceDirect

Journal of Chromatography A

journal homepage: www.elsevier.com/locate/chroma

Application of liquid phase deposited titania nanoparticles on silica spheres to phosphopeptide enrichment and high performance liquid chromatography packings

Jian-Hong Wu [a], Xiao-Shui Li [a], Yong Zhao [b], Weiping Zhang [b], Lin Guo [a,b], Yu-Qi Feng [a,*]

[a] Key Laboratory of Analytical Chemistry for Biology and Medicine (Ministry of Education), Department of Chemistry, Wuhan University, Wuhan 430072, China
[b] College of Life Sciences and State Key Laboratory of Virology, Wuhan University, Wuhan 430072, China

ARTICLE INFO

Article history:
Received 7 September 2010
Received in revised form 25 January 2011
Accepted 12 March 2011
Available online 21 March 2011

Keywords:
Liquid phase deposition
Titania
Phosphopeptide enrichment
Stationary phase
High performance liquid chromatography

ABSTRACT

A novel core–shell composite (SiO_2–*n*LPD), consisting of micrometer-sized silica spheres as a core and nanometer titania particles as a surface coating, was prepared by liquid phase deposition (LPD). Here, we show the resulting core–shell composite to have better efficient and selective enrichment for mono- and multi-phosphopeptides than commercially available TiO_2 spheres without any enhancer. The material exhibited favorable characteristics for HPLC, which include narrow pore size distribution, high surface area and pore volume. We also show that the core–shell composite can efficiently separate adenosine phosphate compounds due to the Lewis acid–base interaction between titania and phosphate group when used as HPLC packings. After coating the silica sphere with titania by LPD, the silanol of silica spheres will be shielded and that the stationary phase, C_{18} bonded SiO_2–3LPD, could be used under extreme pH condition.

1. Introduction

In recent years, the use of titania (TiO_2) and titania-based materials have gained tremendous interest in the field of separation science. In comparison to traditional separation media, these titania-based materials have higher chemical stability, better rigidity, and better amphoteric ion-exchange properties [1–4]. For example, titania–silica composite prepared by co-precipitation has been shown to be more pH stable than silica [5]; titania–zirconia composites synthesized by the sol–gel method showed higher phosphopeptide enrichment efficiency than using single metal oxides [6]. Titania-coated separation materials have been widely used in various separation applications, particularly in high performance liquid chromatography (HPLC) [7–10], capillary electrophoresis (CE) [11–14], and solid-phase microextraction (SPME) [15–18]. Based on the Lewis acid–base interaction between titania and phosphate groups, the use of titania-coated materials has been applied in proteomics and phosphoproteomics [19–22].

Protein phosphorylation is a key regulator of cellular signaling pathways, which is involved in many cellular processes such as proliferation, differentiation and apoptosis [23]. Many proteins with regulatory function are not abundantly expressed, and the stoichiometry of their phosphorylation can be quite low [24]. Thus, phosphorylated protein or peptide enrichment is normally required before they are detected by mass spectrometry. Based on Lewis acid–base interaction, metal oxides such as TiO_2, ZrO_2, Nb_2O_5 and Fe_2O_3 show high selectivity for phosphopeptides enrichment [25–30]. Among these metal oxides, TiO_2 was the most widely used.

To date, most titania-coated materials created so far have been prepared by either the surface sol–gel process (SSP) or by a molecular layer-by-layer self-assembly technique. The surface sol–gel process was originally developed by Kunitake and co-workers [31], and consists of two reactions: (a) non-aqueous condensation of metal-alkoxide precursor molecules with surface hydroxyl groups and (b) aqueous hydrolysis of the adsorbed metal-alkoxide species to regenerate surface hydroxyls [32]. The sol–gel process can occur under mild conditions, and can therefore be used to obtain products in various sizes, shapes and formats [33]. However, as the hydrolysis-polycondensation rate of metal-alkoxide is difficult to control, inevitable coating cracks are produced during the process. The molecular layer-by-layer self-assembly technique is based on the electrostatic attraction between charged species deposited [10,34,35], and a variety of solid substrates may be used, such as latex, inorganic compounds, or metals. The coating generated is thermodynamically stable and can bind firmly to substrates. As a preexisting molecular recognition condition between the materials is required for the molecular layer-by-layer self-assembly technique, this method is limited in its application.

In our study, a simple thin film preparation method was used to prepare novel titania-based materials. In 1988, Nagayama and col-

* Corresponding author. Tel.: +86 27 68755595; fax: +86 27 68755595.
E-mail address: yqfeng@whu.edu.cn (Y.-Q. Feng).

0021-9673/$ – see front matter © 2011 Elsevier B.V. All rights reserved.
doi:10.1016/j.chroma.2011.03.019

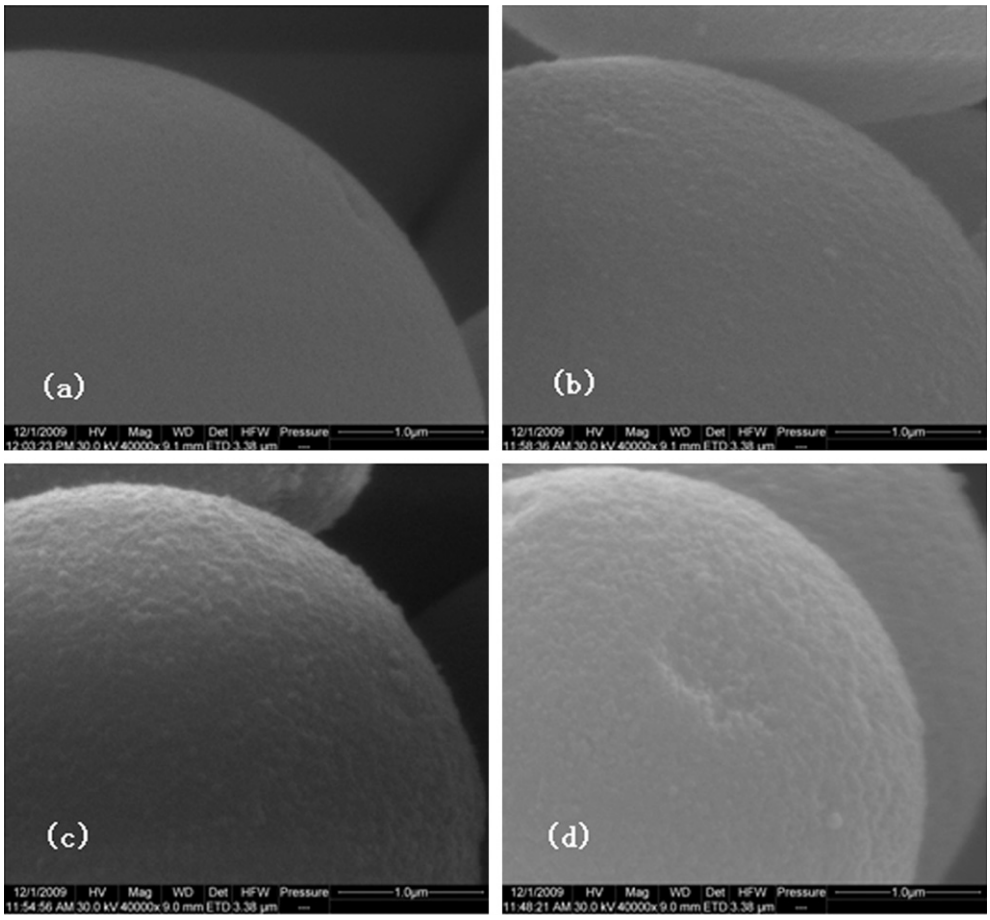

Fig. 1. SEM images of (a) SiO_2 spherical particles, (b) SiO_2–1 LPD, (c) SiO_2–2 LPD, and (d) SiO_2–3LPD.

leagues proposed a simple and environmentally friendly method for producing surface coating fabrication by liquid phase deposition (LPD) [36]. The methodology for the formation of oxide thin films from an aqueous solution in which a metal-fluoro complex is slowly hydrolyzed by adding water, boric acid (H_3BO_3) or aluminum metal. The addition of water directly forces the precipitation of the metal oxide, while boric acid and aluminum act as fluoride scavengers, and act to destabilize the fluoro complex and facilitate oxide precipitation [37]. The inherent advantages of this process are: (a) low cost, (b) nanoparticles are deposited, (c) the available option of adjusting the chemical and physical properties of the obtained oxide films by altering the experimental parameters, (d) strong adhesion of the coating to the substrate provided by chemical bonding. This procedure has been widely used for the preparation of thin films in integrated circuits, metal oxide semiconductors and biosensors. Recently, work from our group has shown that stable titania/silica nanoparticle-coated capillaries prepared by LPD can be used as an extraction media by introducing into in-tube solid phase microextraction (in-tube SPME) [18,38]. In the current study, we report that titania nanoparticles can be used to coat the inner core of micrometer-scale silica spheres by LPD. The resulting core–shell composite was used as the matrix and showed favorable phosphopeptide extraction and chromatographic separation.

2. Experimental

2.1. Chemicals and materials

Fused-silica capillaries with 100 μm I.D. × 365 μm O.D. were from Yongnian Fiber Plant (Hebei, China). Silica spheres (5 μm) were from Welch Materials, Inc. (Shanghai, China) and titania spheres (Titansphere, 5 μm) were from GL Sciences Inc. (Tokyo, Japan). Ammonium hexafluorotitanate ($(NH_4)_2TiF_6$), boric acid (H_3BO_3), tris (hydroxymethyl) aminomethane (tris), triethylamine and other chemical reagents were supplied by Shanghai General Chemical Reagent Factory (Shanghai, China), HPLC grade acetonitrile (ACN) was obtained from Fisher Scientific (Pittsburgh, USA). Ammonia hydrate ($NH_3{\cdot}H_2O$, 25%), phosphoric acid (H_3PO_4), trifluoroacetic acid (TFA), 2,5-dihydroxybenzoic acid (2,5-DHB), bovine α-casein and bovine serum albumin and n-octadecyltrichlorosilane were purchased from Sigma–Aldrich (St. Louis, USA). Sequencing grade trypsin was obtained from Promega (Madison, WI, USA). A synthetic phosphopeptide (GSTAENAEYLR, MW 1210) was kindly provided by L.H. Ericsson (Seattle, Washington, USA). Adenosine 5′-monophosphate (AMP), adenosine 5′-diphosphate (ADP) and adenosine 5′-triphophate (ATP) were obtained from Aladdin Chemical Reagent Co. (Shanghai, China). Purified water was obtained with a Milli-Q apparatus (Millipore, Bedford, MA, USA).

2.2. Preparation of peptide mixture

Bovine α-casein and β-casein were made up into stock solutions of 1 mg/mL using milli-Q purified water. Proteins were digested in trypsin (enzyme to substrate ratio of 1:50 (w/w) in 100 mM Tris–HCl pH 8.5) and incubated overnight at 37 °C.

BSA (1 mg) was dissolved in 100 μL of denaturing buffer solution (8 M urea in 100 mM Tris–HCl pH 8.5). The obtained protein solution was mixed with 5 μL of 100 mM tri(2-chloroethyl)phosphate (TCEP) and incubated for 20 min at room temperature to reduce protein disulfide bonding. Iodoacetamide (3 μL of 500 mM stock)

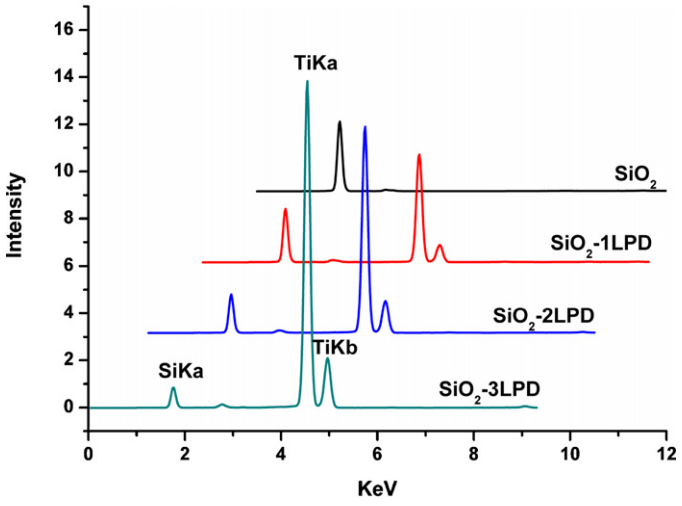

Fig. 2. EDX patterns of SiO_2 and SiO_2–*n*LPD.

was added, and the solution was incubated for an additional 30 min at room temperature in the dark. The reduced and alkylated protein mixture was diluted with 100 mM Tris–HCl pH 8.5. 9 μL of 100 mM $CaCl_2$ was added to produce a total volume of ~50 μL, and the mixture was digested by incubating overnight at 37 °C with trypsin at an enzyme to substrate ratio of 1:50 (w/w).

2.3. Preparation of titania nanoparticle-coated silica particles (SiO_2–nLPD)

The preparative process has three major steps. First, silica spheres were washed with acid and purified water successively, followed by vacuum-drying. Second, the dried silica spheres were incubated in a 100 mL solution containing of 0.1 M $(NH_4)_2TiF_6$ and 0.3 M H_3BO_3 in a PTFE container. After maintaining the spheres under vacuum for 1 h, the mixture was heated at 35 °C for 16 h under continuous shaking. Third, the resulting composite was thoroughly washed with purified water and dried at 120 °C for 4 h. The multilayer titania-coated silica was prepared by repeating the second and third steps several times. The composites were then subjected to heat treatment under air by ramping up to desired temperature at a rate of 1 K/min, and then maintained at constant temperature for 2 h. The resulting composites were denoted as SiO_2–*n*LPD (*n* = deposition time).

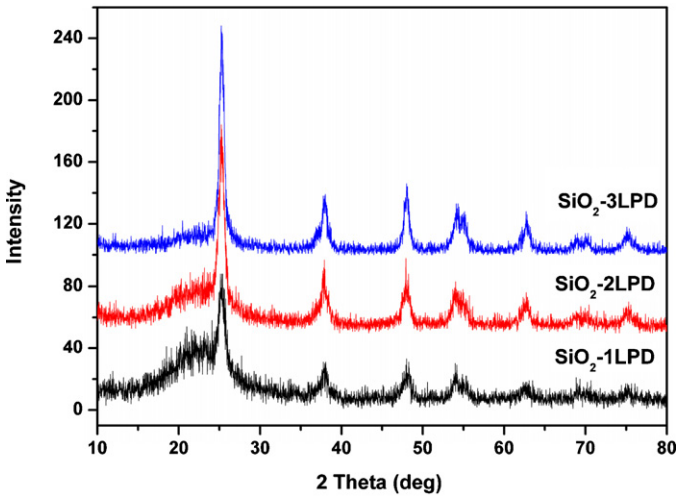

Fig. 3. XRD patterns of SiO_2–*n*LPD.

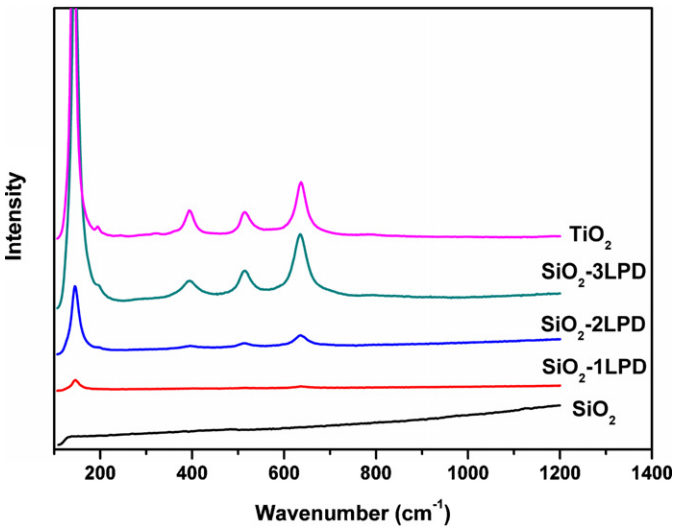

Fig. 4. Raman patterning of SiO_2, SiO_2–*n*LPD and commercially produced TiO_2 spheres.

2.4. Preparation of C18 Bonded SiO_2/SiO_2–3LPD

C_{18} bonded SiO_2/SiO_2–3LPD was prepared according to the method previously reported with minor modification. [39]. Two grams of SiO_2/SiO_2–3LPD were suspended in 40 mL dry toluene and heated to 80 °C, and a toluene solution containing 6 mL/3 mL (24 μmol of silane per m^2 SiO_2/SiO_2–3LPD surface area) and 6 mL/3 mL triethylamine was added. The reaction mixture was stirred for 24 h under reflux at 120 °C, and then, the C18 bonded SiO_2/SiO_2–3LPD was filtered and washed with toluene, followed by washing with acetone and ethanol. The resulting C_{18} bonded SiO_2/SiO_2–3LPD was dried and stored before use.

2.5. Phosphopeptide enrichment procedure

Thirty microliters of peptide solution (in 80% ACN, 1%TFA (v/v)), at various concentrations were used to yield specific amounts of starting material (see Results text). The peptide solution was added to 5 μL of SiO_2–*n*LPD (or commercial TiO_2) slurry (30 mg/mL, in H_2O) and incubated for 30 min by shaking at room temperature, before centrifuging at 15,000 × *g* for 5 min. Particles with bound phosphopeptides were deposited at the bottom of the tube, and the supernatant was removed. The isolated particles were then washed twice with 50 μL solution of 1% TFA containing 80% ACN (v/v) for 30 s to remove nonspecifically adsorbed peptides. The particles were centrifuged at 15,000 × *g* for 5 min, and the supernatant was discarded. The obtained peptide-loaded particles were eluted using 30 μL of 2.5% $NH_3 \cdot H_2O$ (v/v) under agitation for 1 min. The supernatant was collected and 1 μL internal standard solution (GSTAENAEYLR, MW 1210) was added into it. Then the mixture was lyophilized to dryness before MALDI-TOF MS detection.

Table 1
Surface area, pore volume and pore size of SiO_2 and SiO_2–*n*LPD.

	Surface area (m^2/g)	Pore volume (cm^3/g)	Pore size (nm)
SiO_2	375	1.3	11
SiO_2–1LPD	281	1.0	12
SiO_2–2LPD	236	0.8	10
SiO_2–3LPD	146	0.5	12

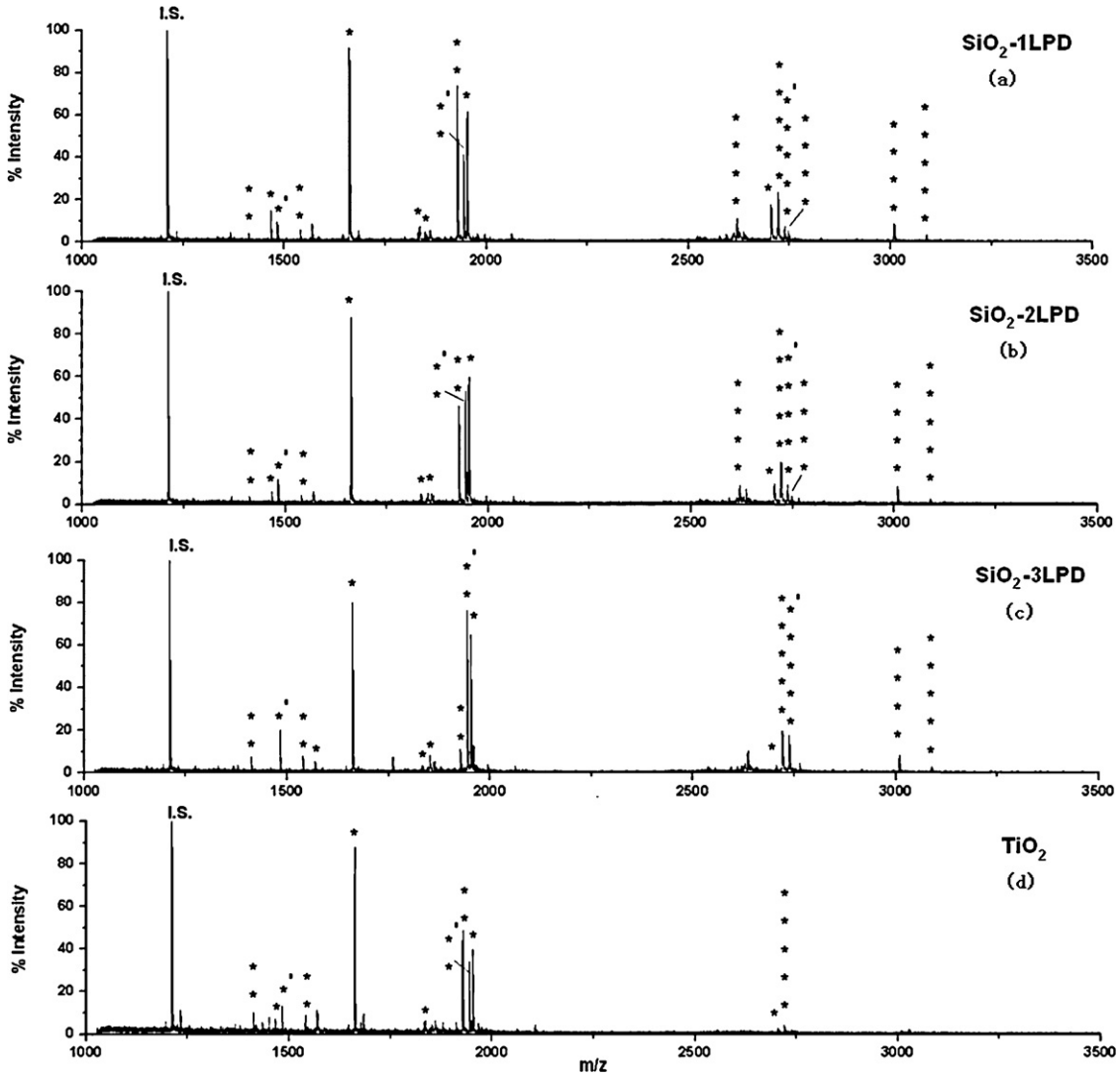

Fig. 5. Mass spectra obtained using the (a) SiO_2–1LPD, (b) SiO_2–2LPD, (c) SiO_2–3LPD and (d) commercial TiO_2 spheres to selectively enrich phosphorylated peptides from tryptic digest of α-casein (1.0×10^{-7} M). The phosphopeptides are marked with asterisks and the number of the asterisks indicates the number of sites phosphorylated. Oxidized phosphopeptides are marked with a quotation mark. The internal standard is marked with "I.S.".

2.6. Instrumentation

SiO_2–*n*LPD spheres were observed with a QUANTA-200 scanning election microscope (SEM, Eindhoven, The Netherlands). The composition of SiO_2–*n*LPD was determined by Shimadzu EDX-720 energy-dispersive X-ray analysis (EDX, Kyoto, Japan) by using Mg Kα radiation as the excitation source. The crystal structure of SiO_2–*n*LPD was determined with a Bruker SMART APEX II X-ray diffractometer (XRD, Billerica, German) using Cu Kα radiation and a rotating anode operated at 40 kV and 30 mA. Raman spectra were collected by Confocal Renishaw Raman Microspectroscopy RM-1000 (London, England). The 514.5 nm line from an Ar^+ laser was used as an excitation source. The power used for commercial TiO_2 and SiO_2–*n*LPD were 0.4 mW and 4 mW, respectively. Nitrogen adsorption measurements were performed at 77 K using a JW-BK surface area and pore size analyzer (JWGB Sci. & Tech., Beijing, China). The composites were activated under vacuum and heated to 393 K for 2 h to remove any physically adsorbed substances before analysis. The specific surface area value was calculated according to the BET (Brunauer–Emmett–Teller) equation at P/P_0 between 0.05 and 0.2. The pore parameters (pore volume and pore diameter) was evaluated from the desorption branch of the isotherm based on BJH (Barrett–Joyner–Halenda) model.

All matrix-assisted laser desorption/ionization time of flight mass spectrometry (MALDI-TOF MS) spectra of the peptides were recorded with a Voyager DE STR MALDI-TOF work station mass spectrometer (Applied Biosystems Inc., USA). During a typical analysis, 200 scans were collected and were performed in positive ion reflector mode with an accelerating voltage of 20 kV and delayed extraction of 280 ns. Two microliters of matrix solution (mixture of 20 mg/mL 2,5-DHB in 50% (v/v) ACN, 1% (v/v) phosphoric acid) was introduced into the eluate and 1 μL of the mixture was used for MALDI-TOF analysis.

2.7. Chromatographic conditions

The μHPLC system consisted of a Shimadzu LC-20AD nano pump, a GL Science MU-701 UV–VIS detector with a 6 nL cell, and a Shimadzu FCV nano Flow Channel Selection Valve. The HPLC apparatus was purchased from Shimadzu (Kyoto, Japan) which consists of two LC-20AD pumps, a SPD-M20A detector, a SIL-20A auto sampler, a CTO-20AC column oven, a DGU-20Ai degasser and a CBA-20A communication bus module. Chromatograms were recorded with Shimadzu LC workstation. All capillary columns were packed at 10 MPa pressure using home-made apparatus. For HPLC column the chromatographic packing (2.0 g) was suspended in 15 mL iso-

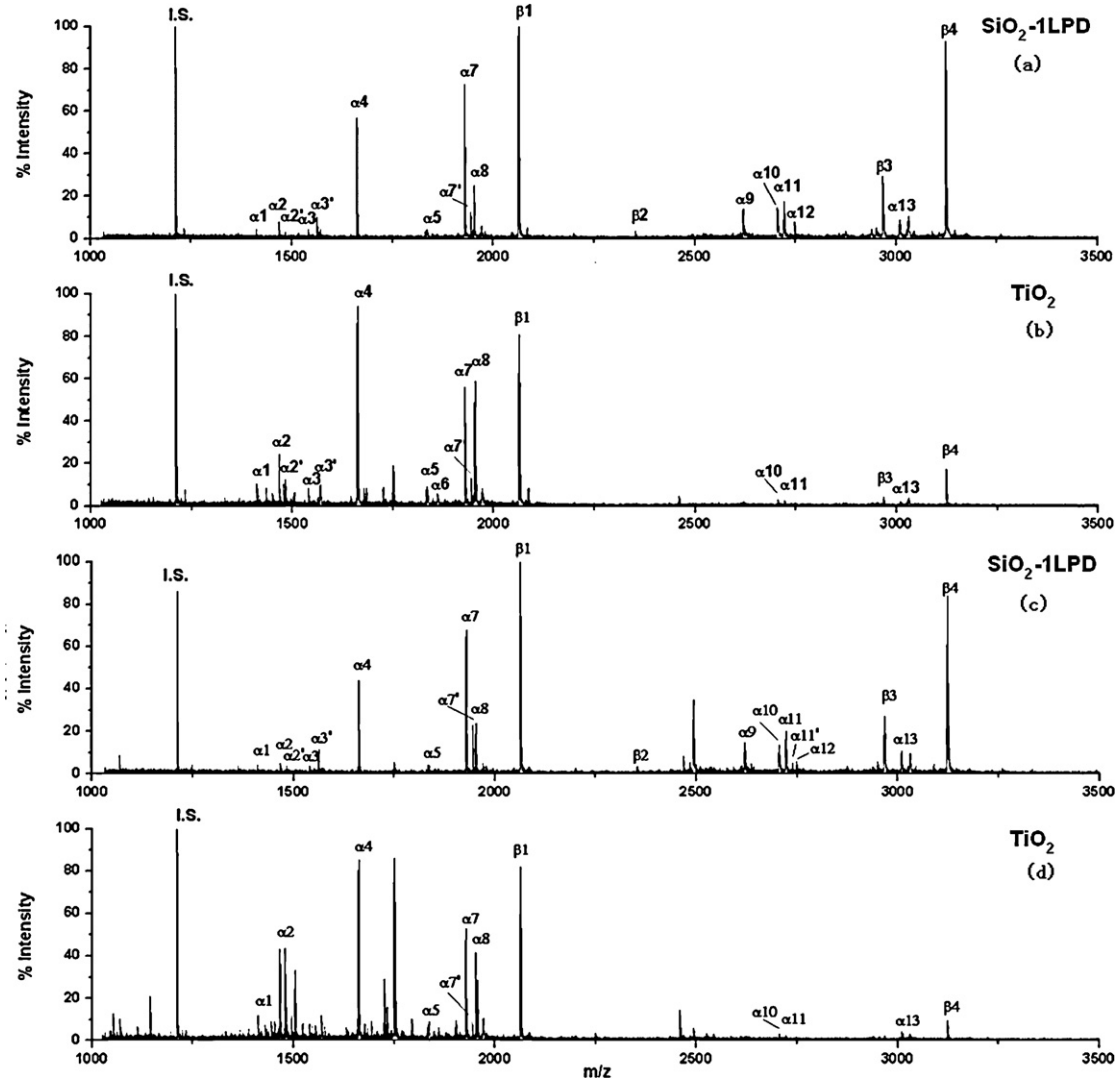

Fig. 6. Mass spectra obtained from SiO_2–1LPD (a, c) and commercial TiO_2 spheres (b, d) enrichment of phosphorylated peptides from tryptic digests of α-casein, β-casein and BSA. The ratios used were 1:1:1 (a, b) and 1:1:10 (c, d). Oxidized phosphopeptides are marked with a quotation mark. The internal standard is marked with "I.S.".

propanol and was ultrasonicated for 15 min to eliminate air and ascertain homogenization. The slurry was packed into a stainless-steel column (150 mm × 4.6 mm i.d.) with methanol as packing solvent under 40 MPa pressure.

3. Results and discussion

3.1. Characterization of SiO_2–nLPD spheres

To characterize the physical properties of SiO_2–*n*LPD particles, the spheres were directly observed by scanning electron microscopy (Fig. 1). The surface of the bare silica (Fig. 1a), and the surface of titania nanoparticle-deposited silica after 1–3 repetitions of the LPD process are shown in Fig. 1b–d. Here, we found small titania particles were formed on the silica substrate after the first round of deposition (Fig. 1b). For dense uniform film formation, a minimum of at least three LPD coatings is required (Fig. 1d).

EDX was performed to examine whether titania particles were present on the silica surface. We show that with increasing coating times, the overall intensity of titanium increased while individual peak height of silicon gradually decreased, this indicates that the titania nanoparticle coating showed increased thickness with increasing coating times (Fig. 2). The analysis data showed that the ratio of Ti/Si is 74.62/25.36 (wt%) when the coating time is 3.

As an HPLC packing material, titania particle chromatographic behavior has been shown to be influenced by the crystalline structure deposited on the surface of silica [40]. The X-ray diffraction spectrum of bare SiO_2 produced a single broad signal demonstrating its amorphous state. In contrast, SiO_2–*n*LPD produced several sharp peaks (Fig. 3), which represents a high degree crystalline structure. Furthermore, the crystallinity of SiO_2–*n*LPD increased with extending coating times. In SiO_2–3LPD, signals corresponding to the tetragonal phase were only observed. By using Scherrer's formula, the grain size of titania particles on SiO_2–*n*LPD was estimated to be ~13 nm, suggesting that the titania nanoparticle coating became more dense with increased coating times.

Raman spectra of the commercial TiO_2, SiO_2 and SiO_2–*n*LPD were obtained (Fig. 4). The spectra of the commercial TiO_2 and SiO_2–3LPD were typical of the anatase TiO_2 phase, but with the peaks widened and a spectral shift comparing to those of single-crystal. Five peaks at the same wave number were observed in Raman spectra of commercial TiO_2, SiO_2–1LPD, SiO_2–2LPD and SiO_2–3LPD, with the peak heights gradually increasing with increasing coating times. The three Raman peaks at 142, 195 and 637 cm^{-1} are assigned to the E_g modes of anatase phase and the Raman peak at 393 cm^{-1} to the B_{1g} mode. The peak at 515 cm^{-1} is a doublet of the A_{1g} and B_{1g} modes. The lowest-frequency E_g mode at 142 cm^{-1} was the strongest of all the observed modes, and is

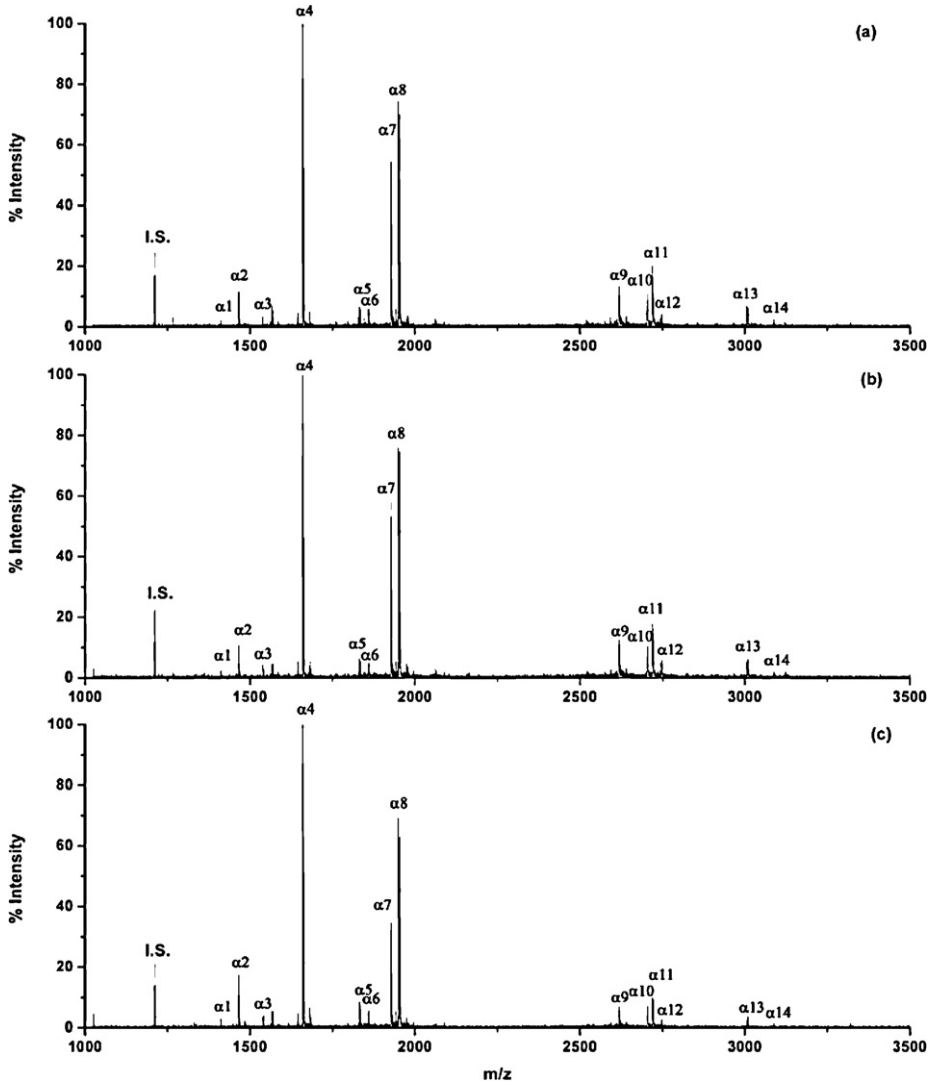

Fig. 7. Mass spectra obtained using the SiO_2–1LPD calcined at (a) 300 °C, (b) 500 °C and (c) 800 °C spheres to selectively enrich phosphorylated peptides from tryptic digest of α-casein (1.0×10^{-7} M). The internal standard is marked with "I.S.".

close to the frequency ($144\,cm^{-1}$) found in the anatase phase of the single-crystal. The measured Raman spectra showed that the TiO_2 nanoparticles deposited on SiO_2 were well crystallized in the anatase structure, which is similar to those found in commercial TiO_2 spheres (Fig. 4).

A comparison of the surface area, pore volume and pore size distribution of bare SiO_2 and SiO_2–*n*LPD is provided in Table 1. Of the four materials, bare silica has the largest surface area as the surface area of SiO_2–*n*LPD decreases with each additional coating. The decrease in the pore volume of the composites is attributable to nanoparticles partly occupying the pore on the surface of bare silica. The pore size distribution of SiO_2–*n*LPD is narrow depending on the narrow pore size distribution of bare SiO_2.

3.2. Phosphopeptide enrichment with SiO_2–nLPD spheres

Multiple-phosphorylated peptide enrichment has been a challenge in phosphoproteomic analysis as these peptides are lowly abundant and extremely hydrophilic, and are not very compatible with mass spectrometry-based analysis operated in the positive ion mode. In order to test the phosphopeptide enrichment properties of SiO_2–*n*LPD, tryptic digests of bovine α-casein (3 pmol) were used in our experiments. α-casein tryptic digest mixtures are abundant in phosphopeptides, particularly peptides with multiple phosphorylation sites. α-casein protein digests were separated with SiO_2–*n*LPD resulting in multiple phosphopeptides were enriched and resolved (Fig. 5). By comparing our results with commercially available TiO_2 spheres from GL sciences (Japan), SiO_2–*n*LPD yielded a stronger signal-to-noise ratio for the multi-phosphopeptides and provided strong confirmation of the identities of the phosphopeptides (Fig. 5).

When more complex protein samples were used, high selectivity towards phosphopeptide is crucial for any enrichment material. Tryptic digest mixtures of α-casein, β-casein and non-phosphoprotein bovine serum albumin (BSA) at ratios of 1:1:1 and 1:1:10 were pretreated with SiO_2–*n*LPD or TiO_2 spheres and the enriched peptides were analyzed by MALDI-TOF MS (Fig. 6). Good signal-to-noise ratios for both mono-phosphopeptides and multi-phosphopeptides were observed for SiO_2–1LPD, while TiO_2 spheres showed somewhat lower recovery for multi-phosphopeptides. For clarity, the observed phosphopeptides detected in our study and their amino-acid sequences are listed in Table 2.

Recently, various kinds of TiO_2 and TiO_2-based materials have been widely used for phosphopeptides enrichment. The capacity of TiO_2 or TiO_2-based materials to capture phosphopeptides can be attributed to the Lewis acid–basic interaction between phosphate groups and Ti ions. The enrichment efficiency of these materials are affected by the coordination environment of the Ti species, crys-

Table 2
Details of the observed tryptically digested α-casein and β-casein phosphopeptides detected by MALDI-MS.

No.	$[M+H]^+$	Phosphorylation site	Amino acid sequence
α_1	1411.1	2	EQLSTSEENSK
α_2	1466.6	1	TVDMESTEVFTK
α_3	1539.7	2	EQLSTSEENSKK
α_4	1660.8	1	VPQLEIVPNSAEER
α_5	1832.9	1	YLGEYLIVPNSAEER
α_6	1847.7	1	DIGSESTEDQAMEDIK
α_7	1927.7	2	DIGSESTEDQAMEDIK
α_8	1952.0	1	YKVPQLEIVPNSAEER
α_9	2619.0	4	NTMEHVSSSEESIISQETYK
α_{10}	2703.5	1	LRLKKYKVPQLEIVPNSAEERL
α_{11}	2720.9	5	QMEAESISSSEEIVPNSVEQK
α_{12}	2747.1	4	NTMEHVSSSEESIISQETYKQ
α_{13}	3008.0	4	NANEEEYSIGSSSEESAEVATEEVK
α_{14}	3088.0	5	NANEEEYSIGSSSEESAEVATEEVK
β_1	2061.8	1	FQSEEQQQTEDELQDK
β_2	2352.9	4	NVPGEIVESLSSSEESITR
β_3	2966.2	4	ELEELNVPGEIVESLSSSEESITR
β_4	3122.3	4	RELEELNVPGEIVESLSSSEESITR

talline, surface area, and Ti content [21,41–43]. SiO_2–*n*LPD have the same crystalline and similar surface areas as the commercial TiO_2 [41]. The formation of titania by LPD can be represented as Eqs. (1) and (2):

$$[TiF_6]^{2-} + 2H_2O \Leftrightarrow TiO_2 + 4HF + 2F^- \quad (1)$$

$$H_3BO_3 + 4HF \Leftrightarrow HBF_4 + 3H_2O \quad (2)$$

$$SiO_2 + HF \Leftrightarrow H_2SiF_6 + H_2O \quad (3)$$

Due to the presence of HF in the solution, small amount of SiO_2 on the silica sphere surface would be dissolved and then re-deposited together with TiO_2 (Eq. (3)). Therefore, by increasing deposition times, Si content on the sphere surface would gradually decrease. As SiO_2–1LPD showed the best enrichment efficiency for multi-phosphorylated peptides, this indicated that a small amount of Si on the SiO_2–1LPD surface may be enough to affect overall phosphopeptide isolation and elution. It is possible that all the phosphate groups of multi-phosphorylated peptides adsorbed on the excess binding site of commercial TiO_2 and were difficult to elute.

It was reported that the calcined titania-based enrichment showed higher selectivity and worse recovery for phosphopeptides [44]. The absorption efficiency of SiO_2–1LPD calcined at 300 °C, 500 °C and 800 °C were compared. As shown in Fig. 7, 14 phosphopeptides were detected in all the mass spectra obtained using the SiO_2–1LPD spheres calcined at 300 °C, 500 °C or 800 °C to selectively enrich phosphorylated peptides from tryptic digest of α-casein. However, the ratio of the intensity of multi-phosphorylated peptides to the internal standard, such as α7, α9 and α11 was slightly decreased when the SiO_2–1LPD was calcined at 800 °C. The results indicate calcined treatment temperature of SiO_2–1LPD has little effect on the selectivity for the phosphopeptides. And the recovery of phosphopeptides was decreased when calcined SiO_2–1LPD (800 °C) was used as phosphopeptides adsorbent. In addition, it was reported the TiO_2 film prepared by liquid phase deposition (LPD) cracked after the thermal treatment at 600 °C, which leaded to the cleavage of surface–film interaction [45]. Therefore, high calcined temperature was not applied in the preparation of SiO_2–*n*LPD.

3.3. Separation of adenosine phosphate compounds on SiO_2–3LPD

Titania-based materials have been widely used as HPLC packings and applied in the separation of adenosine phosphate compounds

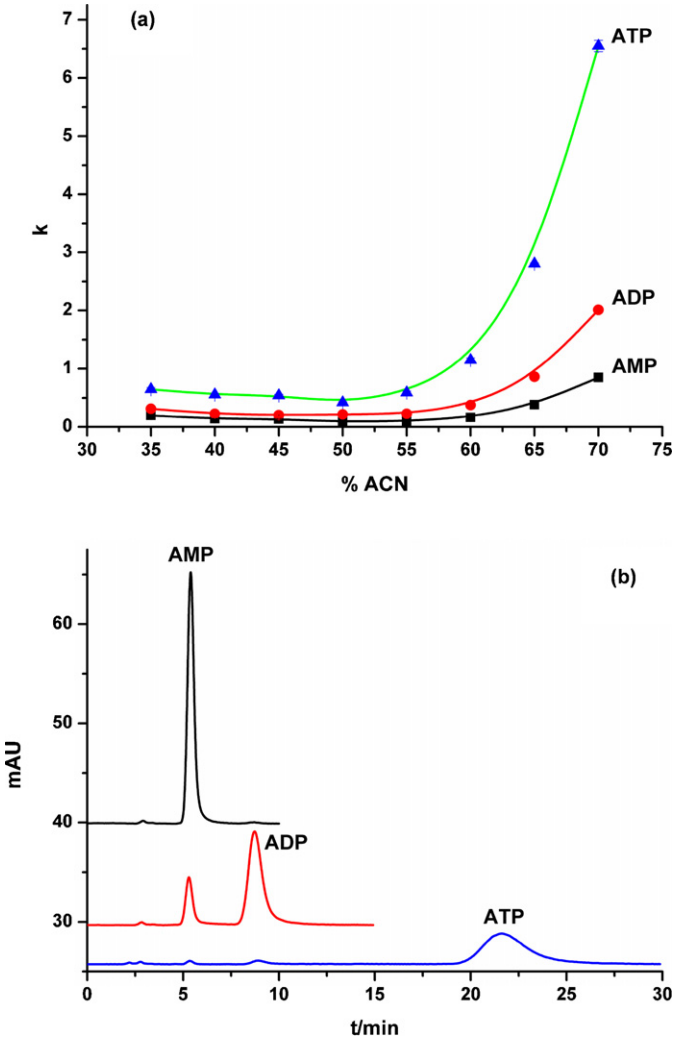

Fig. 8. (a) Effect of different ACN concentrations on retention. (b) Nano-HPLC chromatograms of AMP, ADP and ATP (mobile phase: 70% ACN (v/v) containing 5 mM PBS at pH 7.0). Conditions: flow rate, 400 nL/min; analyte, 40 nL, 0.1 mg/mL AMP, ADP and ATP in the moblie phase; UV detection 254 nm.

[46,47]. SiO_2–3LPD spheres were packed in a capillary column and used as a stationary phase for μHPLC separation of AMP, ADP and ATP. The separation behavior of these adenosine phosphate compounds were investigated using a mobile phase of 70% ACN (v/v) containing 5 mM phosphate buffer (PBS) at pH 7.0. The ACN content in the mobile phases investigated was less than 70% (v/v) due to the low solubility of sodium phosphate in ACN. The retention of AMP, ADP and ATP increased as the ACN content was increased from 50 to 70%, indicating that the separation process was similar to those found in hydrophilic interaction chromatography (HILIC) (Fig. 8a). The retention time increased with the number of the phosphate groups (Fig. 7b). SiO_2–3LPD column exhibited good separation efficiency for adenosine phosphate compounds due to the Lewis acid–base interaction between titania and phosphate group (Fig. 8b).

One of the most significant properties of chromatographic packing is its stability at extreme pH. The frit for capillary column was fabricated with sodium silicate, which might be dissolved at higher pH. In order to investigate the stability of the SiO_2–3LPD, a stainless-steel column (150 mm × 4.6 mm i.d.) was packed with SiO_2–3LPD. The stability test for SiO_2–3LPD stationary phase was carried out at ambient temperature by passing ACN:NaOH solution (70:30, v/v, pH 12) through the column at 1.5 mL/min to a total of 600 column

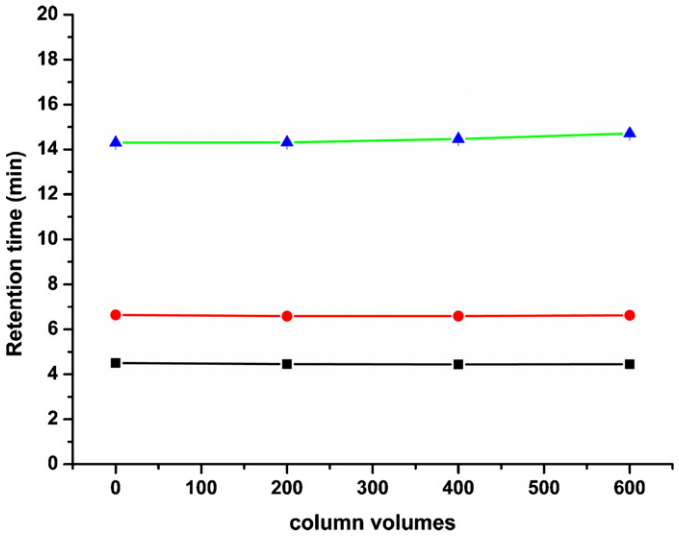

Fig. 9. Retention stability of adenosine phosphate compounds on SiO_2–3LPD: (■) AMP; (●) ADP; (▲) ATP.

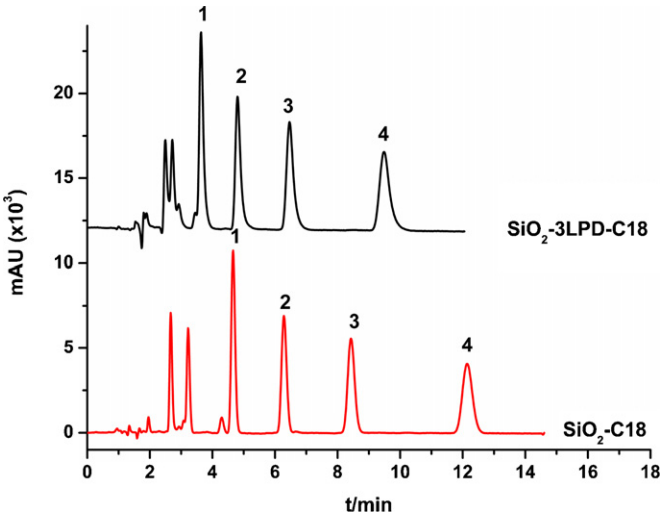

Fig. 10. Chromatograms of four neutral compounds (mobile phase: 50% ACN (v/v), column: SiO_2–3LPD-C18 150 mm × 4.6 mm (i.d.); mobile phase: 60% ACN (v/v), column: SiO_2-C18 150 mm × 4.6 mm (i.d.)). Conditions: flow rate, 1 mL/min; UV detection 254 nm. 1: benzene; 2: toluene; 3: ethylbenzene; 4: n-propylbenzene.

volumes. After passing each 200 column volumes of the alkaline solution, retention time of adenosine phosphate compounds were measured with the mobile phase ACN: PBS at pH 7.0 (67:33, v/v), at a flow rate of 0.75 mL/min (Fig. 9). The relative standard deviations of the retention time for the three compounds were found to be 0.63%, 0.39% and 1.31% respectively, implying that SiO_2–3LPD is stable up to pH 12. In order to investigate the reproducibility of batch-to-batch of the packings, two stainless-steel columns (150 mm × 4.6 mm i.d.) were packed with SiO_2–3LPD spheres from different batches, and AMP, ADP and ATP were used as test compounds. The relative standard deviations of their retention time measured with the mobile phase ACN: PBS at pH 7.0 (67:33, v/v) at a flow rate of 1.5 mL/min were found to be 1.06%, 0.90% and 0.13% respectively, indicating that the reproducibility of batch-to-batch of the packings was satisfactory.

The permeability of the SiO_2–3LPD column (150 mm × 4.6 mm i.d.) was investigated with ACN: PBS at pH 7.0 (67:33, v/v) as mobile phase at a flow rate of 1.5 mL/min. The back pressure of the column was found to be 8.96 Mpa that correspond to the permeability of $K = (uL/\Delta P)\eta = 1.56 \times 10^{-14}$ m^2. This result suggests that the size distribution of the silica particles did not change markedly after the treatment of liquid phase deposition.

Our results indicate that titania nanoparticles can be successfully deposited onto the surface of bare silica sphere by the LPD method. The overall matrix has good mechanical strength and narrow particle distribution due to the silica cores, and the resulting core/shell composite can be applied for HPLC packings.

3.4. Reversed-phase HPLC performance of C_{18} bonded SiO_2–3LPD

To further investigate the chromatographic property of SiO_2–3LPD, it was modified with n-octadecyltrichlorosilane (SiO_2–3LPD-C18) and served as the reversed-phase stationary phase. For comparison, n-octadecyltrichlorosilane modified silica (SiO_2-C18) was prepared in the similar way.

A solution containing benzene, toluene, ethylbenzene, and n-propylbenzene were used as test sample. As shown in Fig. 10, the retention time of the four analytes increased with the increased number of $-CH_2$-groups, demonstrating that C_{18} bonded SiO_2–3LPD/SiO_2 is a good reversed-phase material. Table 3 shows the theoretical plate number and tailing factor for the test compounds. Compared to SiO_2-C18 column, the peaks of the four neutral compounds exhibited tailing on SiO_2–3LPD-C18 column. These results may be due to the change of pore structure after coating the silica sphere with titania nanoparticles.

It has been reported that silica-based packing may adsorb basic compounds through the silanol interaction, which would lead to asymmetric peak [48,49]. After coating the silica sphere with titania by LPD, the silanol will be shielded. In order to demonstrate that the titania shell can effectively shield silanol interactions, the separation behavior of phenol and pyridine was investigated on the SiO_2–3LPD-C18 and SiO_2-C18, respectively. As shown in Fig. 11, pyridine was eluted from SiO_2-C18 column after phenol, while the revered peak order was found on SiO_2–3LPD-C18, indicating that the surface silanol of silica was shielded effectively by LPD titania nanoparticles. Fig. 12 shows the separation behavior of four basic compounds on SiO_2–3LPD-C18 and SiO_2-C18, respectively. Compared to neutral compounds, the tailing factors of basic compounds increased on the both columns. However, the increase in tailing factor on SiO_2-C18 was greater than that on SiO_2–3LPD-C18 column (Table 3).

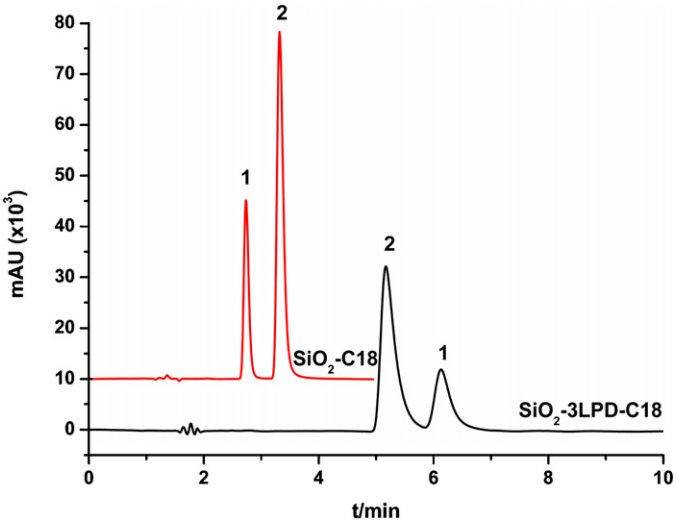

Fig. 11. Chromatograms of phenol and pyridine (mobile phase: 15% ACN (v/v), column: SiO_2–3LPD-C18 150 mm × 4.6 mm (i.d.); mobile phase: 50% ACN (v/v), column: SiO_2-C18 150 mm × 4.6 mm (i.d.)). Conditions: flow rate, 1 mL/min; UV detection 254 nm. 1: phenol; 2: pyridine.

Table 3
Theoretical plate number and tailing factor of the different compounds used.

Column	Compound							
	Benzene	Toluene	Ethylbenzene	n-Propylbenzene	Pyridine	o-Methylaniline	N-methylaniline	N,N-dimethylaniline
SiO_2–3LPD-C18								
N (/m)	22,000	25,000	26,000	27,000	13,000	16,000	25,000	30,000
Tailing F.	1.56	1.51	1.43	1.37	2.10	2.05	1.54	1.34
SiO_2–C18								
N (/m)	38,000	41,000	42,000	42,000	15,000	35,000	38,000	41,000
Tailing F.	1.19	1.13	1.13	1.14	2.21	1.23	1.99	1.16

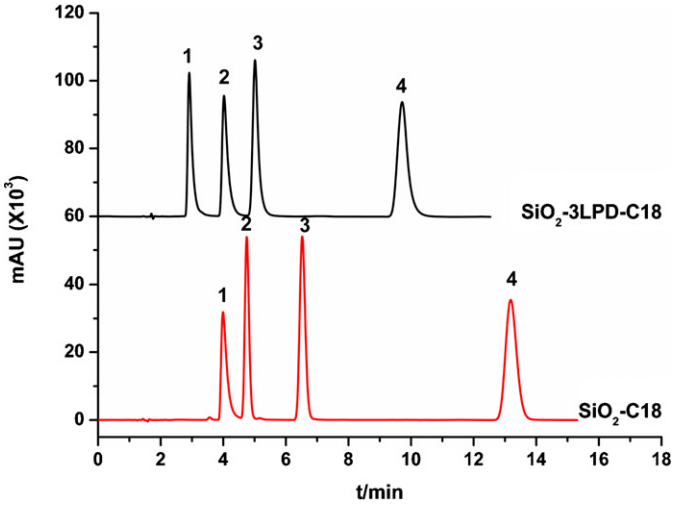

Fig. 12. Chromatograms of four basic compounds (mobile phase: 35% ACN (v/v), column: SiO_2–3LPD-C18 150 mm × 4.6 mm (i.d.); mobile phase: 45% ACN (v/v), column: SiO_2-C18 150 mm × 4.6 mm (i.d.)). Conditions: flow rate, 1 mL/min; UV detection 254 nm. 1: pyridine; 2: o-methylaniline; 3: N-methylaniline; 4: N,N-dimethylaniline.

Most of commercially available silica-based reversed phase chromatography packings are usually required to be used at the pH range of 2–8. Due to the titania shell of SiO_2–3LPD-C18 packing, it was expected that SiO_2–3LPD-C18 could be used under extreme pH condition. The stability test for SiO_2–3LPD-C18 packing was carried out by passing ACN:tris (aqueous, pH 10.1) (35:65, v/v) mobile phase through a column at flow rate of 1.0 mL/min to a total of 1000 column volumes. After passing each 200 column volumes, the retention of test compounds was measured on SiO_2–3LPD-C18. As shown in Fig. 13, very little variation of the retention time (RSD = 0.27% for pyridine, 0.54% for o-methylaniline, 0.57% for N-methylaniline and 0.76% N,N-dimethylaniline) was observed during the investigation. In addition, no shape change of the peaks was observed. These results suggest that SiO_2–3LPD-C18 can be used under extreme pH condition.

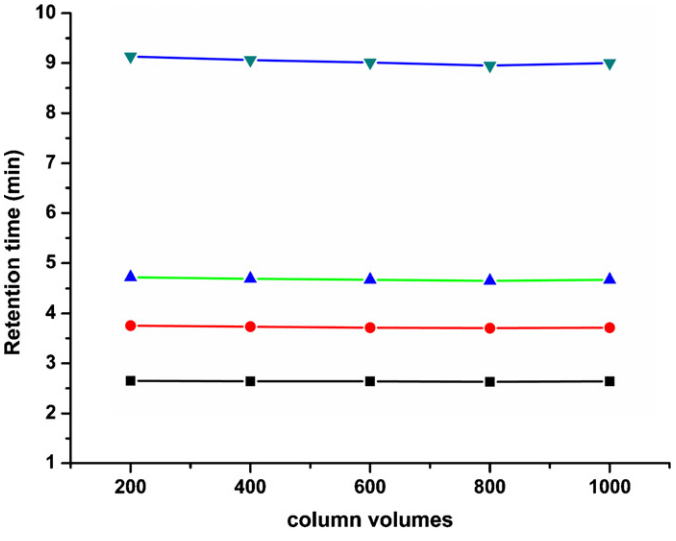

Fig. 13. Retention stability of basic compounds on SiO_2–3LPD-C18: (■) pyridine; (●) o-methylaniline; (▲) N-methylaniline; (▼) N,N-dimethylaniline.

4. Conclusions

In this work, the liquid phase deposited technique was used to produce TiO_2 nanoparticle multilayers on a SiO_2 core and we show that the resulting core–shell composite can be used to efficiently and selectively enrich for both mono-phosphopeptides and multi-phosphopeptides. When used as HPLC packings, the core–shell composite showed a strong ability to separate adenosine phosphate compounds and can effectively avoid adsorption for basic compounds.

Acknowledgements

We would like to thank Ms. Min Zhang (Shimadzu (Shanghai) Co., Ltd.) for EDX analysis and Dr. Barry Wong (Wuhan University) for reading the manuscript. This work was supported by grants from the National 973 project of China (2007CB914200), the National Science Fund for Distinguished Young Scholars (no. 20625516), and the Science Fund for Creative Research Groups (no. 20921062).

References

[1] K. Tani, Y. Suzuki, J. Chromatogr. A 722 (1996) 129.
[2] A. Ellwanger, M.T. Matyska, K. Albert, J.J. Pesek, Chromatographia 49 (1999) 424.
[3] Z.T. Jiang, Y.M. Zuo, Anal. Chem. 73 (2001) 686.
[4] K. Tani, T. Sumizawa, M. Watanabe, M. Tachibana, H. Koizumi, T. Kiba, Chromatographia 55 (2002) 33.
[5] S. Kaneko, S. Ohmori, M. Mikawa, M. Yamazaki, M. Nakamura, S. Yamagiwa, Chem. Lett. (1992) 2249.
[6] J.Y. Yan, X.L. Li, S.Y. Cheng, Y.X. Ke, X.M. Liang, Chem. Commun. (2009) 2929.
[7] R.B. Silva, C.H. Collins, J. Chromatogr. A 845 (1999) 417.
[8] R.B. Silva, K.E. Collins, C.H. Collins, J. Chromatogr. A 869 (2000) 137.
[9] L.S.R. Morais, I.C.S.F. Jardim, J. Chromatogr. A 1073 (2005) 127.
[10] J. Ge, Z.D. Huo, Y.F. Ming, Y.F. Zhao, Y.M. Li, L.R. Chen, Chin. Anal. Chem. 34 (2006) 73.
[11] P. Tsai, C.T. Wu, C.S. Lee, J. Chromatogr. B 657 (1994) 285.
[12] C. Fujimoto, Electrophoresis 23 (2002) 2929.
[13] L. Xu, Y.Q. Feng, Z.G. Shi, S.L. Da, Y.Y. Ren, J. Chromatogr. A 1028 (2004) 165.
[14] Y.L. Hsieh, T.H. Chen, C.Y. Liu, Electrophoresis 27 (2006) 4288.
[15] T.Y. Kim, K. Alhooshani, A. Kabir, D.P. Fries, A. Malik, J. Chromatogr. A 1047 (2004) 165.
[16] S.S. Segro, Y. Cabezas, A. Malik, J. Chromatogr. A 1216 (2009) 4329.
[17] Y. Wu, B. Hu, W. Hu, Z.C. Jiang, B. Li, J. Mass Spectrom. 42 (2007) 467.
[18] B. Lin, T. Li, Y. Zhao, F.K. Huang, L. Guo, Y.Q. Feng, J. Chromatogr. A 1192 (2008) 95.
[19] C.T. Chen, Y.C. Chen, Anal. Chem. 77 (2005) 5912.
[20] Y. Li, X.Q. Xu, D.W. Qi, C.H. Deng, P.Y. Yang, X.M. Zhang, J. Proteome Res. 7 (2008) 2526.
[21] J.J. Wan, K. Qian, L. Qiao, Y.H. Wang, J.L. Kong, P.Y. Yang, B.H. Liu, C.Z. Yu, Chem. – Eur. J. 15 (2009) 2504.
[22] F. Torta, M. Fusi, C.S. Casari, C.E. Bottani, A. Bachi, J. Proteome Res. 8 (2009) 1932.

[23] T.E. Thingholm, O.N. Jensen, M.R. Larsen, Proteomics 9 (2009) 1451.
[24] M. Mann, S.E. Ong, M. Gronborg, H. Steen, O.N. Jensen, A. Pandey, Trends Biotechnol. 20 (2002) 261.
[25] A. Schmidt, E. Csaszar, G. Ammerer, K. Mechtler, Proteomics 8 (2008) 4577.
[26] N. Sugiyama, T. Masuda, K. Shinoda, A. Nakamura, M. Tomita, Y. Ishihama, Mol. Cell. Proteomics 6 (2007) 1103.
[27] G.T. Cantin, T.R. Shock, S.K. Park, H.D. Madhani, J.R. Yates, Anal. Chem. 79 (2007) 4666.
[28] H.J. Zhou, R.J. Tian, M.L. Ye, S.Y. Xu, S. Feng, C.S. Pan, X.G. Jiang, X. Zhou, H.F. Zhou, Electrophoresis 28 (2007) 2201.
[29] S.B. Ficarro, J.R. Parilh, N.C. Blank, J.A. Marto, Anal. Chem. 80 (2008) 4606.
[30] Y. Li, Y.C. Liu, J. Tang, H.Q. Lin, N. Yao, X.Z. Shen, C.H. Deng, P.Y. Yang, X.M. Zhang, J. Chromatogr. A 1172 (2007) 57.
[31] I. Ichinose, H. Senzu, T. Kunitake, Chem. Mater. 9 (1997) 1296.
[32] W.F. Yan, B. Chen, S.M. Mahurin, E.W. Hagaman, S. Dai, S.H. Overbury, J. Phys. Chem. B 108 (2004) 2793.
[33] A. Kumara, Gaurava, A.K. Malika, D.K. Tewary, B. Singh, Anal. Chim. Acta 610 (2008) 1.
[34] H. Dun, W. Zhang, Y. Wei, X. Song, Y. Li, L. Chen, Anal. Chem. 76 (2004) 5016.
[35] X. Liang, S. Wang, J. Niu, X. Liu, S. Jiang, J. Chromatogr. A 1216 (2009) 3054.
[36] H. Nagayama, H. Honda, H. Kawahara, J. Electrochem. Soc. 135 (1988) 2013.
[37] T.P. Niesen, M.R. De Guire, J. Electroceram. 6 (2001) 169.
[38] T. Li, J. Xu, J.H. Wu, Y.Q. Feng, J. Chromatogr. A 1216 (2009) 2345.
[39] K. Kailasam, M.M. Natile, A. Glisenti, K.J. Muller, J. Chromatogr. A 1216 (2009) 2989.
[40] Y. Zhang, C. Chen, H.Q. Qin, R.A. Wu, H.F. Zou, Chem. Commun. 12 (2010) 2271.
[41] K. Imami, N. Sugiyama, Y. Kyono, M. Tomita, Y. Ishirama, Anal. Sci. 24 (2008) 161.
[42] J. Tang, P. Yin, X.H. Lu, D.W. Qi, Y. Mao, C.H. Deng, P.Y. Yang, X.M. Zhang, J. Chromatogr. A 1217 (2010) 2179.
[43] S. Miyazaki, M.Y. Miah, K. Morisato, Y. Shintani, T. Kuroha, K. Nakanishi, J. Sep. Sci. 28 (2005) 39.
[44] K. Imami, N. Sugiyama, Y. Kyono, M. Tomita, Y. Ishihama, Anal. Sci. 24 (2008) 161.
[45] M. Mallak, M. Bockmeyer, P. Löbmann, Thin Solid Films 515 (2007) 8072.
[46] T. Zhou, C.A. Lucy, J. Chromatogr. A 1187 (2008) 87.
[47] J. Konishi, K. Fujita, K. Nakanishi, K. Hirao, K. Morisato, S. Miyazaki, M. Ohira, J. Chromatogr. A 1216 (2009) 7375.
[48] A. Kurganov, T. Trudinger, T. Isaeva, K. Unger, Chromatographia 42 (1996) 217.
[49] Q.H. Zhang, Y.Q. Feng, S.L. Da, Anal. Sci. 15 (1999) 767.